

Retraction

Retracted: Seismic Performance and Vibration Control of Rapid Construction Environmental Protection Wall Based on Artificial Intelligence

International Transactions on Electrical Energy Systems

Received 19 September 2023; Accepted 19 September 2023; Published 20 September 2023

Copyright © 2023 International Transactions on Electrical Energy Systems. This is an open access article distributed under the Creative Commons Attribution License, which permits unrestricted use, distribution, and reproduction in any medium, provided the original work is properly cited.

This article has been retracted by Hindawi following an investigation undertaken by the publisher [1]. This investigation has uncovered evidence of one or more of the following indicators of systematic manipulation of the publication process:

- (1) Discrepancies in scope
- (2) Discrepancies in the description of the research reported
- (3) Discrepancies between the availability of data and the research described
- (4) Inappropriate citations
- (5) Incoherent, meaningless and/or irrelevant content included in the article
- (6) Peer-review manipulation

The presence of these indicators undermines our confidence in the integrity of the article's content and we cannot, therefore, vouch for its reliability. Please note that this notice is intended solely to alert readers that the content of this article is unreliable. We have not investigated whether authors were aware of or involved in the systematic manipulation of the publication process.

Wiley and Hindawi regrets that the usual quality checks did not identify these issues before publication and have since put additional measures in place to safeguard research integrity.

We wish to credit our own Research Integrity and Research Publishing teams and anonymous and named external researchers and research integrity experts for contributing to this investigation.


The corresponding author, as the representative of all authors, has been given the opportunity to register their agreement or disagreement to this retraction. We have kept a record of any response received.

References

- [1] J. Fu, S. Zhou, L. Liu, and M. Liu, "Seismic Performance and Vibration Control of Rapid Construction Environmental Protection Wall Based on Artificial Intelligence," *International Transactions on Electrical Energy Systems*, vol. 2022, Article ID 1385774, 8 pages, 2022.

Research Article

Seismic Performance and Vibration Control of Rapid Construction Environmental Protection Wall Based on Artificial Intelligence

Jie Fu ^{1,2}, Shuangxi Zhou,^{1,2} Li Liu,² and Mingxing Liu^{1,2}

¹Jiangxi Key Laboratory of Disaster Prevention-mitigation and Emergency Management, East China Jiaotong University, Nanchang 330013, Jiangxi, China

²School of Civil Engineering and Architecture, East China Jiaotong University, Nanchang 330013, Jiangxi, China

Correspondence should be addressed to Jie Fu; 2928@ecjtu.edu.cn

Received 18 August 2022; Revised 5 September 2022; Accepted 17 September 2022; Published 29 September 2022

Academic Editor: Nagamalai Vasimalai

Copyright © 2022 Jie Fu et al. This is an open access article distributed under the Creative Commons Attribution License, which permits unrestricted use, distribution, and reproduction in any medium, provided the original work is properly cited.

With the continuous increase in building types, people's demand for buildings is increasing. In addition to focusing on the work of the building itself, high requirements are also placed on the safety, stability, and durability of the building. Especially in other earthquake-prone areas, it is even more necessary to strengthen seismic isolation research to reduce vibration. Rapid construction of environmental protection walls pays attention to environmental protection and efficiency during construction, which can effectively solve problems in the construction process, but the seismic resistance of rapid construction environmental protection walls is unknown. Therefore, this paper used artificial intelligence technology to study the seismic performance of rapid construction environmental protection walls and analyzed its vibration control. This paper firstly established the seismic performance analysis model of the environmental protection wall, used the finite element method to construct the environmental protection wall model, and then used the artificial intelligence algorithm to analyze the seismic performance of the rapid construction environmental protection wall. The experimental results showed that the peak load of the rapid construction environmental protection wall was about 250 KN, and the seismic performance was good.

1. Introduction

In the design of the seismic isolation layer of the building structure, the design work is generally completed in the way of the superstructure, the intermediate isolation layer, and the substructure. The design mode of the seismic isolation layer can better improve the use efficiency of the superstructure, avoid the abnormality of the superstructure, and ensure that it can still maintain a good elastic effect after the earthquake's destructive force. In addition, in the process of seismic isolation layer design, its strength should be comprehensively analyzed in combination with relevant parameters such as building structure, construction area environment, and geological conditions. It is necessary to ensure that the seismic energy would not have a bad effect on the overall application effect of the structure. The research

on the seismic performance and vibration control of building walls can maintain the comprehensive application quality of building structures and reduce safety hazards and economic losses, so it is very necessary to test the seismic performance of building walls.

At present, there are many studies on the seismic performance and vibration control of buildings. Varum gave a detailed description of the seismic performance of buildings in Nepal [1]. Sabermahany and Attarnejad compared the seismic response of shallow hyperbolic shell raft foundations supported by steel flexural structures with those of these structures supported by piled raft foundations [2]. Bento and Simoes summarized the research status of seismic performance evaluation of buildings [3]. Sovester and Adiyanto investigated the performance of a reinforced concrete school building in Sabah that suffered multiple earthquakes [4].

Verma and Ram conducted a review of building standard guidelines that were important in preventing various types of damage typical of seismic conditions [5]. Although there are many studies on the seismic performance and vibration control of buildings, there are few studies on the seismic performance of rapid construction environmental protection walls.

Artificial intelligence has been used in construction. Roslon used artificial intelligence and hyper-heuristic algorithms to select materials and techniques during construction in a way that improves project parameters [6]. Liang et al. used artificial intelligence to predict internal heat gain in ventilation and air conditioning [7]. Zhi used blockchain and artificial intelligence to build smart cities [8]. Abioye et al. revealed AI applications, examined AI technologies in use, and identified opportunities and challenges for AI applications in the construction industry [9]. Hooda et al. studied how artificial intelligence and its various principles can be integrated with the emerging field of structural engineering [10]. Although artificial intelligence has many applications in construction, it has not been used to detect the seismic performance of buildings.

This paper used artificial intelligence technology to study the seismic performance of rapid construction of environmental protection walls. In this paper, finite element analysis software was used to establish the seismic performance analysis model of the environmental protection wall, and then artificial intelligence technology was used to identify the seismic performance of the wall, and the vibration control method is analyzed. In the experimental part, experiments were carried out on the wall from five aspects: load-displacement relationship, stiffness degradation curve, plastic rotation angle, shear deformation angle in the core area of nodes, and interstorey displacement ductility coefficient to study its seismic performance.

2. Model of Seismic Performance of Environmental Protection Wall

The research object of this paper is the problem of computational fracture methods because the failure limit is a process of energy change as the crack evolves and propagates. At the same time, due to the appearance of cracks, the material is in a state of failure and the area shows non-uniformity. The finite element program ANSYS has a powerful function of calculating crack structures, so this program is used for finite element calculation and analysis of walls [11].

The local element failure method was developed based on the principle of continuous failure mechanism. If the element that reaches the critical damage value looks like a crack, the whole process of cracking and fracturing can be analyzed with clear physical meaning.

ANSYS software integrates the Solid65 rigid body 3D model mainly used for concrete, which is convenient for users to calculate the final concrete proportion. The Solid65 tool itself has two parts. One part is based on the Solid45 eight-point entity combination, which takes into account the properties of concrete, adding a concrete failure model and a

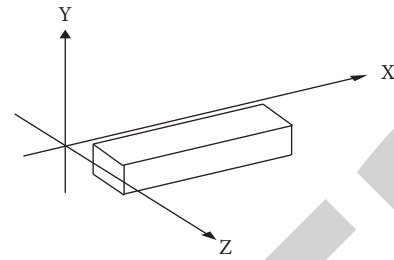


FIGURE 1: The Link8 space rod unit.

distribution model under triaxial stress. The other part is a model consisting of diffuse rebar elements. In the model, the material, position, angle, and reinforcement ratio of the reinforcement are set by entering actual parameters. Since the discrete model is used in this paper, there is no need to reinterpret the diffusion coefficient element [12].

Another important feature of the Solid65 material is the propagation crack model. Due to the high tensile strength of the material, concrete members in many cases suffer from cracks, which cause sudden changes in local stress and stiffness. In finite element analysis, there are three main methods for dealing with cracks. It includes comparing individual cracks with element boundaries, comparing distributed cracks with internal relationships, and modifying element design functions to construct basic element models.

2.1. The Type of Unit Used

2.1.1. Rod Unit. Rebar analysis in ANSYS usually adopts 2-node 3d bar elements such as Link1, Link8, Link180, beam element Beam188, and pipe element Pipe20. In this paper, the Link8 rod unit is selected, which only bears axial tension and compression and has no correction time. It has 3 directions and can be used to study various mechanical problems such as elasticity, plasticity, creep, expansion, and large deformation [13]. The Link8 pole module is shown in Figure 1.

2.1.2. Brittle Material Element (Solid65). At the loading and support points of the part, to avoid a single concentration of pressure, causing undue breakage, and difficult integration, it needs to increase the required size or add soft spots. The elastic pad uses Solid45 material, and by defining a large elastic modulus, a force or constraint is applied to the elastic pad, and the pressure is transmitted through the elastic pad. The brittle material unit is shown in Figure 2.

Due to the complex design of the computational model, there are many applications. In order to facilitate the step-by-step densification of the spatial cell grid and have a strong realization in the design, the cell type shown in Figure 2(c) is adopted in this paper.

2.1.3. Concrete Unit (Solid92). Concrete elements are used to model reinforced concrete materials. Solid92 is a ten-node tetrahedron model with high precision. The ten-node tetrahedron element has a strong correlation with the shape,

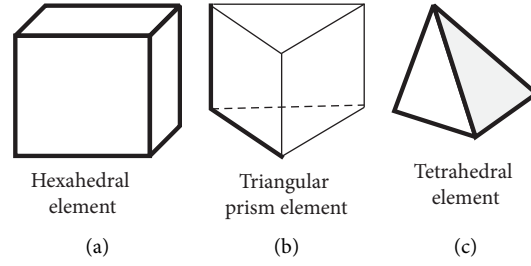


FIGURE 2: The brittle material unit (a) is a hexahedral unit, (b) is a triangular prism unit, and (c) is a tetrahedral unit.

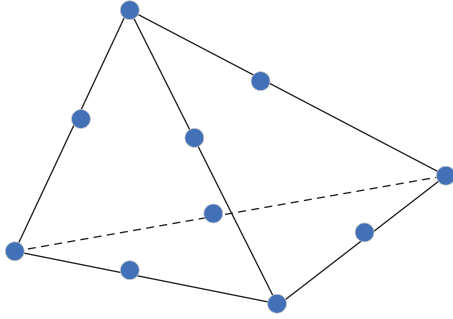


FIGURE 3: The ten-node tetrahedral element.

which is convenient for the gradual refinement of the space grid [14]. The ten-node tetrahedral element is shown in Figure 3.

2.2. Finite Element Mesh Division. There are two methods of meshing, one is the method of defining nodes and creating elements. One is to create an instance of the instance, and after the instance is created, the network is directly mapped to the instance. This paper adopts the latter method. After a model is created, there are two ways to mesh it: a free mesh method and a regular mesh method. The free grid method has a good way of adapting to complex boundaries, while the regular grid method has high requirements on the geometric boundaries of the model. Or it can be said that if the normal meshing method is used, the model needs to take special treatment [15]. This article would use the free meshing method.

2.3. Determination of Wall Analysis Model. The three solid parameters of the relevant material are described below [16].

2.3.1. Wall Tie Bars. The steel bar (a typical elastic-plastic material) can be simulated by imitating the plastic steel bar model, and the $\Phi 6$ -type tension bar is subjected to a uniaxial tensile test on the universal testing machine, and the simplified stress-strain curve is obtained.

2.3.2. Reinforced Concrete Components. Reinforced concrete members are composite elastic-plastic materials. If this is converted to a homogeneous material, the material parameters in the elastic plane can be calculated exactly as follows:

$$E = \frac{E_1 V_1 + E_2 V_2}{V_1 + V_2} \quad (1)$$

In the formula, E_1 is the elastic modulus of the steel bar and V_1 is the total volume of the steel bar in the member. E_2 is the elastic modulus of concrete and V_2 is the volume of concrete.

Similarly, the yield stress of the same member should also be calculated equivalently as follows:

$$\sigma_s = \frac{\sigma_1 V_1 + \sigma_2 V_2}{V_1 + V_2} \quad (2)$$

σ_1 is the yield stress of steel bars and σ_2 is the yield stress of concrete.

After a component enters the plastic stage, it can be considered to satisfy the following rules:

$$\sigma = A \varepsilon^{1/4} \quad (3)$$

The stress-strain curve of reinforced concrete can be calculated.

2.3.3. Masonry. The masonry conforms to the law of elastic-brittle deformation. The strength of the block measured by the test is 13 MPa, and the strength of the mortar is 7 MPa. The formula for the compressive strength of masonry is

$$f_m = 0.78 \sqrt{f_1 (1 + 0.07 f_2)} \quad (4)$$

The formula for tensile strength of masonry is as follows:

$$f_{t,m} = K_3 \sqrt{f_2} \quad (5)$$

Among them, $K_3 = 0.141$.

3. Recognition of Vibration Pattern of Environmental Protection Wall Based on Artificial Intelligence

The intelligent pattern recognition system utilizes the motion signals of different patterns collected at the beginning and uses the network architecture for deep machine learning. It can continuously associate with different motion patterns, and then detect motion patterns in different situations and send messages to the outside world. The method can be used in intelligent motion detection and fault diagnosis and early warning systems to ensure the safe

operation of equipment [17]. It prevents and reduces the occurrence of major accidents. In this paper, by building an intelligent vibration detection system, combined with deep machine learning, it can judge different movement patterns, identify memory and learn more information, and then conduct early warning tests.

3.1. Theoretical Basis of Vibration Pattern Recognition. In this paper, the single-arm optical fiber transmission detection method is adopted. Circulators, fiber probes, reflectors, and other experimental samples were used in the experiments, and the wave Formula of the new optical fiber electromagnetic waveguide is the Maxwell1 Formula. The identification is essentially the solution of the Maxwell1 Formulas [18].

$$\begin{aligned}\nabla \times E &= -\frac{\partial B}{\partial t}, \\ \nabla \times H &= \frac{\partial D}{\partial t} + J, \\ \nabla \times D &= \rho, \\ \nabla \times B &= 0.\end{aligned}\quad (6)$$

Among them, D , B , J , ρ can be expressed as follows:

$$\begin{aligned}D &= \varepsilon E = \varepsilon_0 \varepsilon_r E, \\ B &= \mu H = \mu_0 \mu_r H, \\ J &= 0, \\ \rho &= 0.\end{aligned}\quad (7)$$

The electric field strength is represented by E , the magnetic field strength is represented by H , and the electric displacement is represented by D . The magnetic induction intensity is represented by B , the current density is represented by J , the charge density is represented by ρ , the vacuum permittivity is represented by ε_0 , and the relative permittivity is represented by ε_r .

According to Maxwell's Formulas, the electromagnetic field continuity conditions at the interface of the medium can be obtained as follows:

$$\begin{aligned}n \times (E_1 - E_2) &= 0, \\ n \times (H_1 - H_2) &= 0, \\ n \times (\mu_1 H_1 - \mu_2 H_2) &= 0, \\ n \times (\varepsilon_1 H_1 - \varepsilon_2 H_2) &= 0.\end{aligned}\quad (8)$$

The normal unit vector of the interface is denoted by n , and the permeability is the scalar constant μ .

3.2. The Method of Vibration Pattern Recognition. Specific considerations for finite element analysis are as follows:

The first step determines the field, the second step selects the translation function, and the third step determines the eigenvalues. The fourth step is to create a finite element Formula system, the fifth step is to solve the finite factor

Formulas, and the sixth step is further computational processing [19].

The first step in determining the field is to divide the field into small regions of different shapes, such as 6-sided, 4-sided, and 3-sided. The second step is to choose the interpolation function by function type and then compute the domain scale to solve for the subdomain terms. The third step is to define the eigenvalues, coefficient matrices, interpolation functions, subdomain geometry, and properties of the different problems. The fourth step is to generate the finite element Formula of the system. Specifically, the field value at the node is calculated by computer simulation. In the calculation, a linear Formula system must be generated first. The fifth step in solving the finite element Formulas is to solve the system of linear Formulas and the value of the unknown domain and finally use the interpolation function to solve the value of any point in the domain.

4. Recognition of Vibration Pattern of Environmental Protection Wall Based on Artificial Intelligence

4.1. Active Control Technology. Generally speaking, active control is a vibration reduction control technology that uses other external forces to effectively control the vibration reduction of buildings by using different external vibration reduction control forces. Its working principle consists of four factors [20]:

- (1) Sensors can be used to monitor the external shock and dynamic response of the building structure.
- (2) The target data can be transferred to the computer.
- (3) The energy to be used can be calculated using a calculation method defined by a computer program.
- (4) The energy that can effectively control the system can be generated according to the external energy source.

4.2. Semiactive Control Technology. Generally speaking, semiactive control is the use of control technology to automatically adjust the parameters in the building system to achieve the purpose of effective vibration reduction. This control mode can be effectively accomplished with only a weak current and in the semi-intermediate control technique, switches are used for effective control. The operating state of the system is effectively controlled by various functions on the switch, thus changing the dynamic performance of the building structure to a certain extent.

At present, the typical semiactive control technology devices are variable damping systems, variable stiffness systems, controllable friction system, and parameter active adjustment of the mass damping system.

4.3. Passive Control Technology. Generally, in the vibration control of building structures, passive control generally refers to a technology that does not rely on external forces to control vibration. It adds subsystems to specific areas of the building structure to effectively improve the dynamic characteristics of

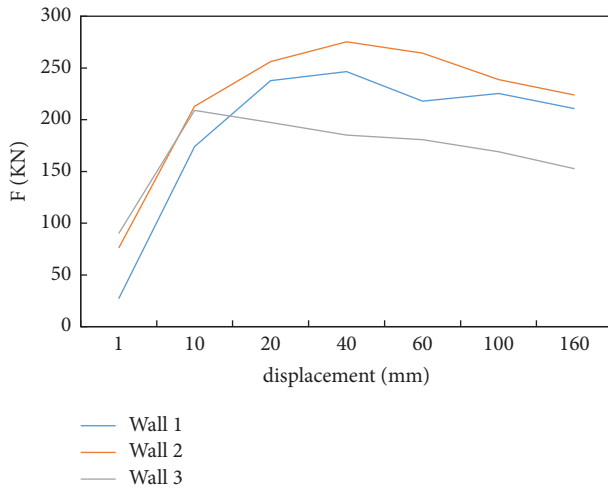


FIGURE 4: The wall load-displacement curve.

the structure itself. It is either set through a series of characteristics of the structure itself on the structural components. This passive control technology of vibration is a popular technology at present, and many passive controls have been perfected and widely used in practical applications.

4.4. Hybrid Control Technology. Hybrid control technology combines active and passive control. Combining the advantages of the two, it can not only destroy a large amount of seismic energy through the control device but also use the active control device to verify the control effect. Therefore, it is very important to use hybrid control in the design process. A general hybrid control device mainly includes a damping energy release device and a hybrid control combination of an active control hybrid device, active control, and a basic isolation device.

4.5. Comprehensive Analysis of Four Technologies. In general, the active control technology is the best among the four technologies, but due to the larger building volume and the need for more external power sources, the algorithm of the control device and system is also very complex, and this technology is less applicable than the other three technologies. Passive control technology has become the most widely used and fastest-growing technology due to its advantages of good vibration reduction, low cost, and easy implementation. The semiactive control technology is between active control and passive control. Compared with active control, it has high control accuracy and relatively low cost and has broad application prospects. The hybrid control technology is the product of multiple control technologies, which combines the advantages of all control technologies, so its development prospect is definitely broader than other control technologies [21].

5. Experimental Results of Wall Seismic Performance

Three types of quick-construction environmentally friendly walls commonly used in the market are selected and named

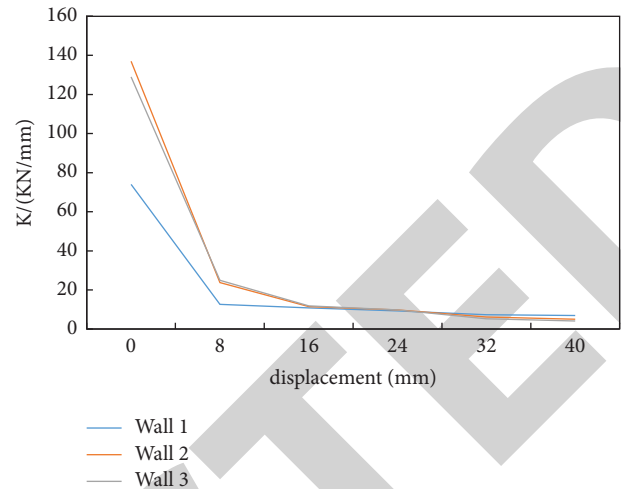


FIGURE 5: Wall stiffness degradation curve.

wall 1, wall 2, and wall 3. In this paper, the seismic performance of the wall is studied from five aspects: load-displacement relationship, stiffness degradation curve, plastic rotation angle, shear deformation angle of node core area, and interstory displacement ductility coefficient.

5.1. Load-Displacement Curve. The load-displacement curves of the three kinds of walls are shown in Figure 4.

Wall 1 reaches the initial crack state when the load is 40 kN and reaches the yield state when the load is 241.5 kN. When the load is 246.5 kN, the wall load reaches its peak value, and when the load decreases to 210.6 kN, the displacement of wall 1 reaches the limit. Wall 2 reaches the initial crack state when the load is 116 kN and reaches the yield state when the load is 219.4 kN. When the load is 275.3 kN, the load of wall 2 reaches its peak value, and when the load decreases to 223.9 kN, the displacement of wall 2 reaches the limit. When the load is 93 kN, wall 3 reaches the initial crack state, and when the load is 184.7 kN, it reaches the yield state. When the load is 209 kN, the load of wall 3 reaches its peak value, and when the load decreases by 152.7 kN, the displacement of wall 3 reaches the limit.

It can be seen from the data that in the initial stage of test loading, the curve shows a straight upward trend, and the stiffness of wall 1, wall 2, and wall 3 is not much different. When cracks appear in the wall, the structural stiffness decreases significantly, but the stiffness of wall 3 decreases the most. After the structure enters the yield state, loads of wall 1 and wall 2 continue to increase with the increase of displacement, but a load of wall 3 quickly reaches the peak value. Compared with wall 3, the descending section of the load-displacement curve of wall 1 and wall 2 is gentler.

On the whole, the peak load of the rapid construction environmental protection wall is about 250 kN.

5.2. Stiffness Degradation Curve. The three kinds of wall stiffness degradation curves are shown in Figure 5.

When there is no crack in the wall, the stiffness of the three kinds of walls is 74 kN/mm, 137 kN/mm, and 129 kN/mm.

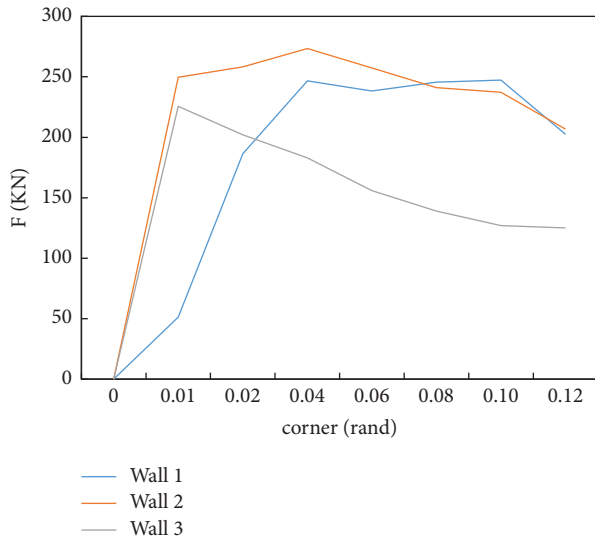


FIGURE 6: The relationship between load and plastic rotation angle.

mm respectively. When the wall crack is 8 mm, the stiffness of wall 1 is 12.6 KN/mm, the stiffness of wall 2 is 23.7 KN/mm, and the stiffness of wall 3 is 24.9 KN/mm. At this stage, the stiffness of the wall decreases sharply. When the wall crack is 16 mm, the stiffness of wall 1 is 10.8 KN/mm, the stiffness of wall 2 is 11.5 KN/mm, and the stiffness of wall 3 is 11.9 KN/mm, and then the stiffness of the wall decreases slowly.

In the early stage of test loading, cracks appeared in the wall and gradually expanded, resulting in a rapid decrease in the ability of the structure to resist horizontal loads and a rapid rate of stiffness degradation. In the later stage of loading, the stiffness degradation curve tends to be flat, indicating that after the wall is fully cracked and damaged, most of them quit work, and the structural stiffness is mainly provided by the frame. The stiffness degradation curves of wall 2 and wall 3 are similar. Compared with wall 2 and wall 3, the stiffness of wall 1 is relatively small, especially in the early stage of loading.

5.3. Plastic Corner. The relationship between load F and the plastic rotation angle is shown in Figure 6.

When the plastic rotation angle is 0.01rand, the load of wall 1 is about 50 KN, and the load of wall 2 and wall 3 is about 250 KN. When the plastic rotation angle is 0.02rand, the load of wall 1 and wall 3 is about 200 KN, and the load of wall 2 is about 250 KN. Then, with the gradual increase of the plastic corner of the wall, loads of wall 1 and wall 2 increase slowly and then gradually decrease, and a load of wall 3 decreases rapidly. When the plastic corner of the wall is 0.12rand, the load of wall 1 and wall 2 is about 200 KN, and a load of wall 3 is 125 KN.

5.4. Shear Deformation Angle in the Core Area of the Node. The relationship between the load F and the shear deformation angle γ in the core area is shown in Figure 7.

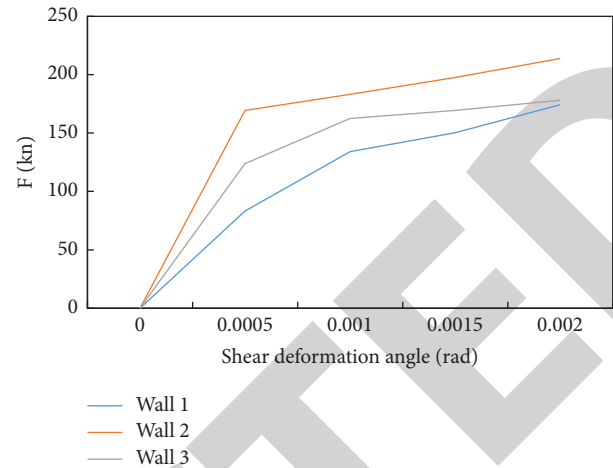


FIGURE 7: The relationship curve of the shear deformation angle of the core area.

TABLE 1: Wall interlayer displacement ductility coefficient.

Wall	Interlayer displacement ductility coefficient
Wall 1	7.4
Wall 2	11.3
Wall 3	8.1

When the wall load is small, the shear deformation angle in the core area of the wall node is very small, only 1/11 to 1/7 of the final shear deformation angle. When a large number of cracks at the column end develop and extend, the shear deformation angle begins to increase significantly, especially after the plastic hinge appears at the column end, and the shear deformation angle increases most significantly. Under the same horizontal load, the shear deformation angles of the core area of the node are wall 2, wall 3, and wall 1 in descending order.

5.5. Interlayer Displacement Ductility Coefficient. The relationship between the displacement ductility coefficients of the three kinds of walls is shown in Table 1.

The interlayer displacement ductility coefficient of wall 1 is 7.4, the interlayer displacement ductility coefficient of wall 2 is 11.3, and the interlayer displacement ductility coefficient of wall 3 is 8.1.

6. Results of Seismic Performance of Rapid Construction Environmental Protection Wall

This paper uses a machine learning algorithm to analyze the seismic performance of rapid construction environmental protection wall and discusses the vibration control method of rapid construction environmental protection walls. The research results are as follows:

- (1) In this paper, the finite element program ANSYS is used to construct the 3D model of the wall, and the element types such as rod element, brittle material element, and concrete element are introduced, and

the tetrahedral element structure is selected as the element type. Then, it builds the wall models and uses the regular mesh method to divide the finite element mesh.

- (2) This paper uses the deep learning method to construct an intelligent pattern recognition system, introduces the theoretical basis of vibration pattern recognition, and introduces the steps of vibration model recognition in detail.
- (3) This paper introduces the vibration control method for the rapid construction of environmental protection walls. It includes active control technology, semiactive control technology, passive control technology, and hybrid control technology, analyzes the control principles, and advantages and disadvantages of the four technologies.
- (4) In the experimental part, this paper selects 3 kinds of rapid construction environmental protection walls on the market. The wall is tested from five aspects: load-displacement relationship, stiffness degradation curve, plastic rotation angle, shear deformation angle of node core area, and interstory displacement ductility coefficient. This paper studies the seismic performance of rapid construction environmental protection walls. For the load-displacement relationship, the peak load of the three kinds of rapid construction environmental protection walls is about 250 KN. For the stiffness degradation curve, in the initial stage of loading, the stiffness degradation rate of the rapid construction environmental protection wall is faster, and with the gradual increase of the load, the stiffness degradation of the wall gradually slows down.

7. Conclusion

This paper uses the finite element method to establish a finite element model for the rapid construction of environmental protection walls and uses artificial intelligence technology to calculate the seismic performance of the wall. In the experiment part, the load-displacement relationship, stiffness degradation curve, plastic rotation angle, shear deformation angle of node core area, and interstory displacement ductility coefficient of rapid construction environmental protection wall were measured. The experimental results show that the rapid construction environmental protection wall has high load capacity and good seismic performance.

Data Availability

No data were used to support this study.

Conflicts of Interest

The authors declare that they have no conflicts of interest.

Authors' Contributions

All authors have seen the manuscript and approved to submit to your journal.

Acknowledgments

This work was supported by the National Natural Science Foundation of China (51968022) and Academic and Technical Leaders of Major Disciplines in Jiangxi Province (20213BCJL22039).

References

- [1] H. Varum, "Seismic performance of buildings in Nepal after the gorkha earthquake," *Impacts and Insights of the Gorkha Earthquake*, vol. 2018, no. 6, pp. 47–63, 2018.
- [2] H. Sabermahany and R. Attarnejad, "Seismic performance of buildings supported by a shallow doubly-curved shell raft foundation," *Structures*, vol. 36, no. 2, pp. 619–634, 2022.
- [3] R. Bento and A. Simoes, "Seismic performance assessment of buildings," *Buildings*, vol. 11, no. 10, pp. 440–453, 2021.
- [4] H. H. Sovester and M. I. Adiyanto, "Seismic performance of reinforced concrete school buildings in sabah," *Malaysian Academic Library Institutional Repository*, vol. 64, no. 8, pp. 148–152, 2017.
- [5] I. Verma and S. Ram, "Effect of irregularities on seismic performance of buildings," *A Review*, vol. 2020, no. 7, pp. 351–369, 2020.
- [6] J. Roslon, "Materials and technology selection for construction projects supported with the use of artificial intelligence," *Materials*, vol. 15, no. 4, pp. 1282–1283, 2022.
- [7] R. Liang, W. Ding, Y. Zandi, A. Rahimi, S. Pourkhorshidi, and M. A. Khadimallah, "Buildings' internal heat gains prediction using artificial intelligence methods," *Energy and Buildings*, vol. 258, no. 7, pp. 111794–112726, 2022.
- [8] Q. Zhi, "The integration of blockchain and artificial intelligence for a smart city," *Academic Journal of Computing & Information Science*, vol. 4, no. 8, pp. 45–63, 2021.
- [9] S. O. Abioye, L. O. Oyedele, L. Akanbi et al., "Artificial intelligence in the construction industry: a review of present status, opportunities and future challenges," *Journal of Building Engineering*, vol. 44, no. 12, pp. 103299–104127, 2021.
- [10] Y. Hooda, P. Kuhar, K. Sharma, and N. K. Verma, "Emerging applications of artificial intelligence in structural engineering and construction industry," in *International Conference on Mechatronics and Artificial Intelligence (ICMAI) 2021*, Gurgaon, India, 27 February 2021.
- [11] W. He, X. He, and C. Sun, "Vibration control of an industrial moving strip in the presence of input deadzone," *IEEE Transactions on Industrial Electronics*, vol. 64, no. 6, pp. 4680–4689, 2017.
- [12] G. Park, "Vibration control using a variable coil-based friction damper," in *Proceedings Volume 10164, Active and Passive Smart Structures and Integrated Systems 2017*, no. 9, pp. 101–105, Portland, OR, USA, 2017.
- [13] C. U. Dogruer and A. K. Pirsoltan, "Active vibration control of a single-stage spur gearbox," *Mechanical Systems and Signal Processing*, vol. 85, no. 2, pp. 429–444, 2017.
- [14] Z. Lu, Z. Wang, Y. Zhou, and X. Lu, "Nonlinear dissipative devices in structural vibration control: a review," *Journal of Sound and Vibration*, vol. 423, no. 3, pp. 18–49, 2018.
- [15] "Draeos," *Deep Learning: Neural-Inspired Artificial Intelligence*, vol. 2017, no. 5, pp. 1308–1320, 2017.
- [16] S. Elias, "Effect of SSI on vibration control of structures with tuned vibration absorbers," *Shock and Vibration*, vol. 2019, Article ID 7463031, 12 pages, 2019.
- [17] R. Atassi and R. Atassi, "Geological landslide disaster monitoring based on wireless network technology," *International*

- Journal of Wireless and Ad Hoc Communication*, vol. 2, no. 1, pp. 21–32, 2021.
- [18] D. Hassabis, D. Kumaran, C. Summerfield, and M. Botvinick, “Neuroscience-inspired artificial intelligence,” *Neuron*, vol. 95, no. 2, pp. 245–258, 2017.
- [19] W. Sun, H. Reza Karimi, S. Yin, and J. M. Rossell, “Active vibration control in mechanical systems,” *Mathematical Problems in Engineering*, vol. 2014, Article ID 275087, 2 pages, 2014.
- [20] D. Ali and S. Frimpong, “DeepImpact: a deep learning model for whole body vibration control using impact force monitoring,” *Neural Computing & Applications*, vol. 33, no. 8, pp. 3521–3544, 2021.
- [21] R. Li, Z. Zhao, X. Zhou et al., “Intelligent 5G: when cellular networks meet artificial intelligence,” *IEEE Wireless Communications*, vol. 24, no. 5, pp. 175–183, 2017.

RETRACTED